

RSscore: Reaction Superiority Learned from Reaction Mapping Hypergraph

Chenyang Xu¹, Lijuan Guo¹, and Lei Zhang¹

¹Dalian University of Technology

October 27, 2023

Abstract

The selection of chemical reactions is directly related to the quality of synthesis pathways, a reasonable reaction evaluation index plays a crucial role in the design and planning of synthesis pathways. Since the construction of traditional reaction evaluation indicators mostly rely on the structure of molecules rather than the reactions themselves, considering the impact of reaction agents poses a challenge for traditional evaluation indicators. In this study, we first propose a chemical reaction graph descriptor that includes the mapping relationship of atoms to effectively extract reaction features. Then, through pre-training using graph contrastive learning and fine-tuning through supervised learning, we establish a model for generating the probability of reaction superiority (RSscore). Finally, to validate the effectiveness of the current evaluation index, RSscore is applied in two applications: reaction evaluation and synthesis routes analysis, which proves that the RSscore provides an important agents-considered evaluation criterion for Computer-Aided Synthesis Planning (CASP).

RSscore: Reaction Superiority Learned from Reaction Mapping Hypergraph

Chenyang Xu, Lijuan Guo, Lei Zhang*

Frontiers Science Center for Smart Materials Oriented Chemical Engineering, Institute of Chemical Process Systems Engineering, School of Chemical Engineering, Dalian University of Technology, Dalian 116024, China

KEYWORDS: Machine learning; Computer-aided synthesis planning; Reaction evaluation indicator; Reaction graph; Graph contractive learning.

ABSTRACT:

The selection of chemical reactions is directly related to the quality of synthesis pathways, so a reasonable reaction evaluation index plays a crucial role in the design and planning of synthesis pathways. Since the construction of traditional reaction evaluation indicators mostly rely on the structure of molecules rather than the reactions themselves, considering the impact of reaction agents poses a challenge for traditional evaluation indicators. In this study, we first propose a chemical reaction graph descriptor that includes the mapping relationship of atoms to effectively extract reaction features. Then, through pre-training using graph contrastive learning and fine-tuning through supervised learning, we establish a model for generating the probability of reaction superiority (RSscore). Finally, to validate the effectiveness of the current evaluation index, RSscore is applied in two applications: reaction evaluation and synthesis routes analysis, which proves that the RSscore provides an important agents-considered evaluation criterion for Computer-Aided Synthesis Planning (CASP).

1. Introduction

Chemical reaction selection and design play a key role in drug and material synthesis.¹ The synthesis conditions (temperature, pressure, solvents, etc.), time and yield of the product can be greatly optimized through selecting an appropriate chemical reaction pathway. Therefore, the design of evaluation indicators for Computer Aided Synthesis Planning (CASP) has evolved in recent years.²⁻⁷ CASP evaluation indicators are mainly divided into two catalogs: expert knowledge-based evaluation indicators^{8,9} and synthesis complexity/accessibility-based evaluation indicators.¹⁰⁻¹⁷ For expert knowledge-based evaluation indicators, the rank of synthesis results are determined by experts.^{8,9} Although this kind of methods have a high confidence level, it still suffers from ambiguity and lack of objectivity. So, it is difficult to be applied in retrosynthesis tasks and provide an objectivity guidance on synthesis route.⁶ For synthesis complexity/accessibility-based evaluation indicators, the feasibility of synthesis is qualified by molecular structures and the reaction relationship between reactants and products.¹⁰⁻¹⁷ Although synthesis complexity/accessibility evaluation indicator eliminates the ambiguity and objectivity problems, the influence of reaction agents and conditions are still unable to be considered in these indicators.

Here, a brief overview of existing synthesis complexity/accessibility-based evaluation indicators is given. SAScore¹³ uses Extended Connectivity Fingerprints (ECFPs)¹⁸ fragment analysis obtained from the compounds of PubChem database¹⁹. According to the frequency of each fragment occurrence, each fragment is assigned a numerical score. After combining the fragment score with the penalty for complexity and the bonus for symmetry, SAScore is able to measure compound synthesis accessibility on a high-throughput scale. SAScore is widely used in guiding synthesis directions in retrosynthesis.^{20,21} Based on the assumption that the complexity of the reactants is lower than products, a data-driven metric SCscore¹⁴ was designed to describe real syntheses. Trained by 22 million reactant-product pairs from the Reaxys²² database, SCscore is able to describe the complexity of the synthetic route.⁴ Although this evaluation metric differs from the metric of synthetic accessibility, it can also be used as a guide for retrosynthesis through the Morgan Fingerprints input. SYBA¹⁵ is a fragment-based method for the rapid classification of the synthesis difficulty of organic compounds. It uses Bernoulli Naïve Bayes classifier to assign SYBA score contributions to individual fragments based on their frequencies in the database of easy- (ES) or hard-to-synthesize (HS) molecules. Although it can be used to quickly rank large molecular datasets for high-throughput screening or molecular design, it still cannot compete with more sophisticated synthetic path reconstruction methods that enable the incorporation of other factors²³. RAScore and GASA are the evaluation metrics using a similar method in retrosynthesis accessibility.^{16,17} Machine Learning (ML) is used in these methods to generate the probability of retrosynthesis accessibility. The data-driven models of RAScore and GASA were trained by using ES or HS labels generated by multistep retrosynthetic planning algorithm such as Retro*²⁴ and AiZynthFinder.²⁵ Although these developed evaluation metrics are able to clearly determine the difficulty of molecular synthesis, the impact of reaction agents is still unable to be considered.

With the development of ML, Graph Neural Networks (GNN) are gradually used in chemistry. In addition to predicting molecular thermodynamic properties in the dataset such as QM9,²⁶⁻²⁹ it has also been used in molecular generation,^{30,31} reinforcement learning for molecular design,³² molecular representation learning³³⁻³⁷ and reaction yield prediction³⁸ in recent years. For the molecular representation learning method, SMILES Contrastive Learning (SMICLR) framework was proposed which embraces multimodal molecular data. It jointly trains a graph encoder and SMILES encoder to perform the contrastive learning. Through data augmentation on graphs and SMILES sequences, SMICLR model successfully reduced the prediction error for the energetic and electronic properties of the QM9 dataset.³³ MolCLR is a self-supervised learning framework which performs graph data augmentation and contrastive learning method on a large unlabeled molecular database to achieve representation learning of molecules. Benefiting from pre-training on a large unlabeled database, MolCLR even achieves state-of-the-art results on several challenging benchmarks after fine-tuning.³⁴GeomGCL designs a novel geometric graph contrastive scheme to enable collaborative supervision between 2D and 3D molecular graph geometric views, aiming to improve model generalization ability on molecular graph classification and regression.³⁵ MoCL is a contrastive learning framework which

utilizes domain knowledge at both local and global levels to learn molecular representations. By replacing valid substructures with bioisosteres that share similar properties, MoCL achieves accurate prediction of molecular properties, providing a suitable and powerful augmentation method for molecular graph.³⁶ KCL builds a knowledge graph data augmentation module by using fundamental chemical attributes to connect atoms that are not directly connected by bonds.³⁷ By using a double MPNN model, extensive experiments demonstrated that KCL obtained superior performance against state-of-the-art baselines on eight molecular datasets, demonstrating the feasibility of the framework for molecular representation learning. In summary, contrastive learning method shows a better performance on molecular properties prediction. It illustrates that contrastive learning method is able to help the model extract more features and improve prediction effect of molecular properties.

In this work, we migrate the generation method of molecular synthesis accessibility to reaction superiority and design a reaction total atom-atom mapping algorithm to complement the atomic mapping relationship in the chemical reaction database. By using the reaction descriptors constructed from the reaction mapping relationships and reaction reagents, a chemical reaction representation learning model is constructed through a contrastive learning method. After fine-tuning the model on a binary classification task for determining reaction superiority, reaction superiority score (RSscore) is generated to evaluate the superiority of chemical reactions and further applied on reaction evaluation and synthesis route analysis.

2. Method

2.1 Overview

In this section, a model framework for generating the probability of reaction superiority (RSscore) is developed. As shown in **Fig. 1**, the proposed framework is divided into 4 parts: (a) Reaction Total Atom-Atom Mapping algorithm; (b) Reaction condense hypergraph generation; (c) Contrastive learning pre-training process and (d) Supervised learning fine-tuning process.

As some unimportant products and some atom mapping relationship are not recorded in Open Reaction Database (ORD)³⁹, to complement the missing products and the atom mapping relationship, Reaction Total Atom-Atom Mapping (RTAAM) algorithm is developed to compensate these information (**Fig. 1(a)**), which provides more reaction features for model and improves prediction accuracy. In part (b), a new condensed hypergraph descriptor is proposed to describe chemical reactions through connecting reaction graph and agent graph using molecular/reaction node (**Fig. 1(b)**). With this descriptor, the information of reactions and agents are integrated into the summary node, at the same time, the influence between reactions and agents can be considered. In part (c), the contrastive learning model is utilized to pre-train the initial parameters of the backbone model in unlabeled reaction data. After data augmentation and contrastive learning model training, the initial parameters of the backbone model are optimized to bring similar reaction features closer together and push different reaction features further apart (**Fig. 1(c)**). In part (d), the parameters of the backbone model and multilayer perceptron (MLP) layers are fine-tuned using supervised learning. After mapping the output values to the interval from 0 to 1 using Sigmoid activation function, the superiority probability of the reaction is generated to evaluate the reactions. (**Fig. 1(d)**)

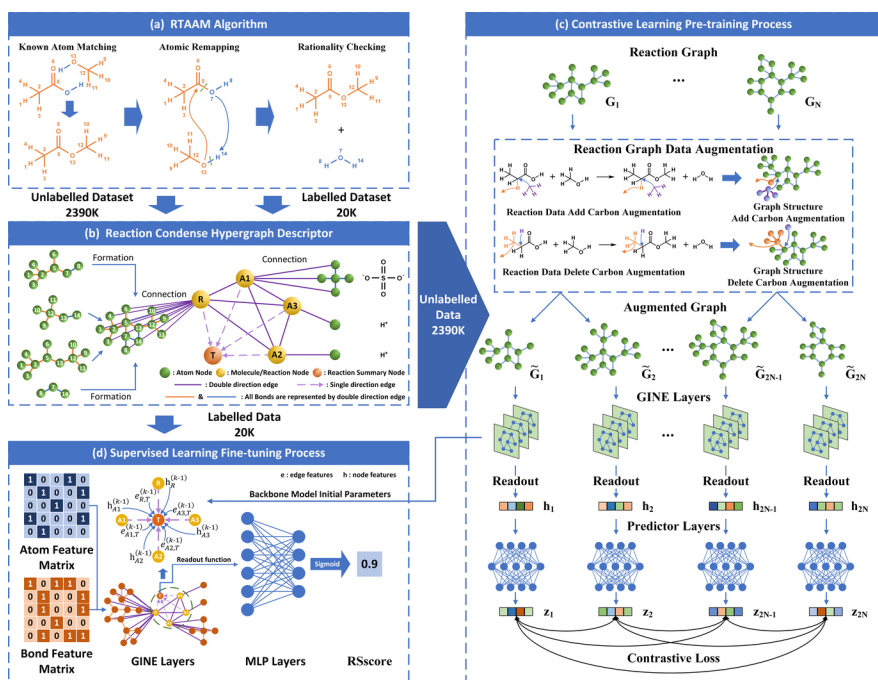


Fig. 1: The overview of RScore model framework

2.2 Dataset preparation

USPTO in ORD database³⁹ is selected as the data source for generating dataset. Since some reactions in the ORD database do not have complete atomic mapping relationships information (such as known atom matching, as the functional group hydroxyl and hydrogen shown in blue in **Fig.1 (a)**), the Reaction Total Atom-Atom Mapping (RTAAM) algorithm are designed to complement atom mapping relations. Moreover, there is no clear boundary between superior and inferior reaction determination, thus label generation and label smoothing are utilized for subsequent model training.

2.2.1 Reaction Total Atom-Atom Mapping (RTAAM) algorithm

In the dataset, unimportant products are not always recorded, which causes not all atoms in the reaction have mapping index. To complement the missing products and the atom mapping relationship, RTAAM algorithm is developed (**Fig 1(a)**). The RTAAM algorithm can be divided into three steps.

Step 1: Known atom mapping. The SMARTS of the missing product is determined during the reaction completion process based on the transfer relationship of the atoms. In the ORD database, the known atomic mapping relationships already exist in the reaction SMARTS, therefore the atomic remapping can be performed after the known atomic mapping relationships identification completed. In cases where atom mapping relationships are absent, the rxnmapper⁴⁰ is used to generate a reasonable mapping to achieve matching of known atoms in the reactions.

Step 2: Atomic remapping. From the atom remapping step for different reaction class in **Fig. 2**, the reaction class and the atom mapping indexes of the missing product can be determined according to the available atom mapping information and the difference of the bond features between the reactants and products. For substitution reactions and elimination reactions, the SMARTS of the missing product is constructed by connecting the missing atomic mapping numbers of the leaving groups directly. For addition reactions and rearrangement reactions, all products have been already recorded in reaction SMARTS. Therefore, the

algorithm only needs to operate on the changes in bonds to infer the atomic mapping relationship. After adding the omitted hydrogen atoms and the corresponding atom mapping relationships, the remapping relationships of reaction atoms can be completed. More details are shown in **Supplementary Information**

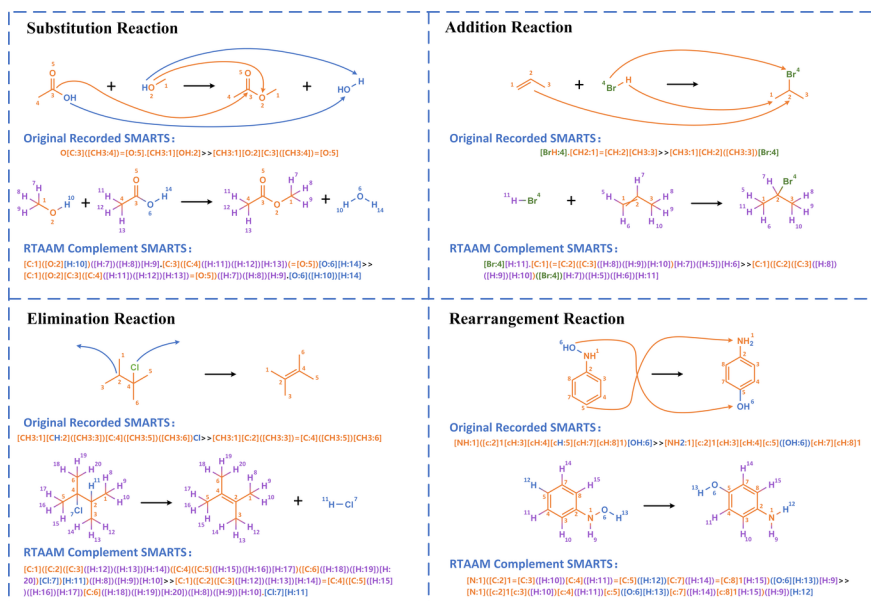


Fig. 2: Atom remapping step in RTAAM algorithm

Step 3: Rationality checking. After completing the supplementation of the missing products and the atom remapping, the properties of the atom connections and reaction rationality checks are required to prevent the generation of unreasonable molecules. For atomic connection check, since some atom's connection situation does not satisfy the rationality during the reaction atomic remapping process, the connection of each atom is checked to make sure all atoms are reasonably connected. When there are only two remaining atoms require an additional single bond connection, the algorithm will directly carry out the connection between two atoms to complete the remapping relationship. For other cases, if the algorithm fails to perform the complement, the reaction will be abandoned. The algorithm also detects whether the redox agent is involved in the reaction to ensure that the mapping relationship of the atoms in the reaction is constructed reasonably.

2.2.2 Labels generation

After deleting the reactions without SMARTS information and/or the reactions failed to perform atom mapping complementation algorithm, 2,397,092 reactions are remained for generating modelling dataset. Since labels are necessary for model construction in supervised learning methods. Thus, labels are assigned to reactions based on thresholds in **Table 2** to classify superior and inferior reactions. Here, 20,000 reactions are selected to assign labels and 1,400 reactions for external testing. The reactions with high reaction yields, short reaction times and mild reaction temperatures are regarded as positive examples, while the reactions with low reaction yields, long reaction times and tough reaction temperature are regarded as negative ones.

Table 2. Reaction superiority classification boundary

Reaction type	High superiority	Low superiority
Reaction yield (%)	90 - 100	0 - 50

Reaction type	High superiority	Low superiority
Reaction time (h)	0.1 - 1.5	> 8
Reaction temperature (°C)	15 - 30	< -10 or > 100
Special cases	-	Yield < 15% and 4h < Time < 12h

To prevent excessively intense reactions or excessively long reaction times under the boundary conditions of reaction time, the upper and lower limits of superior reaction time are set at 0.1h and 1.5h respectively. As for the boundary conditions of reaction temperature, the temperatures near the room temperature are considered as superior reaction temperatures, while temperatures exceeding the boiling point of water and temperatures requiring artificial cooling are considered as inferior reaction ones.

According to the distribution of reaction yields recorded in the ORD database, it can be observed that most of the reaction yield are distributed between 90% and 100% (**Fig. 3**), with only a small portion distributed below 50%. Therefore, we set the upper and lower boundaries for yield as 90% and 50% respectively to enhance differentiation between variations. Furthermore, reactions with notably low yields and reasonably moderate reaction times are also classified as inferior reactions.

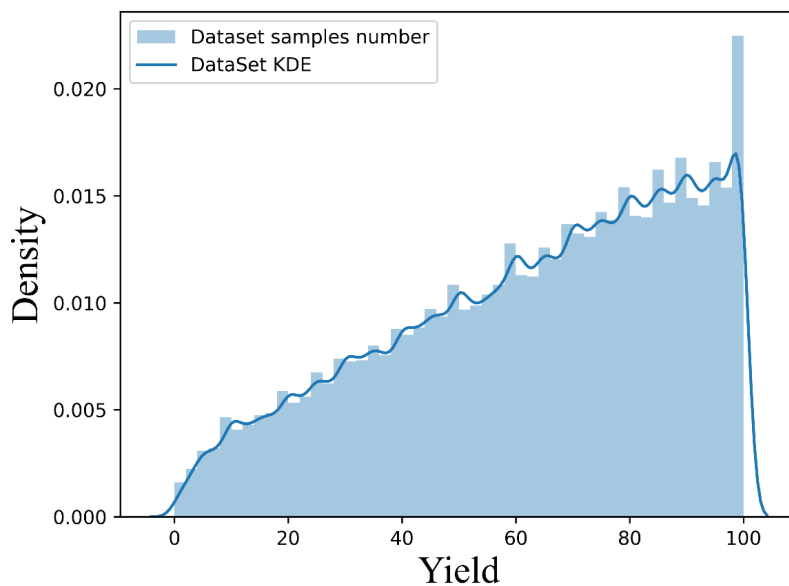


Fig. 3. The kernel density estimation curve of ORD yield

2.2.3 Labels smoothing

To address the limitation of traditional binary label encoding in describing reaction superiority within the same label category, label smoothing methods are employed to differentiate between varying degrees of reaction superiority and reduce overfitting during model training. In this case, the superiority labels for 20,000 reactions in the fine-tuning dataset are reconstructed based on the assumption that the overall effects of reaction yield, time and temperature conditions are the uniform and linear. According to the compensation part equations provided in **Table 3**, the high superiority reactions labels are remapped to a range of 0.85 to 1.0, and the low superiority reaction labels are remapped to a range of 0.0 to 0.15.

Table 3. Compensation equations in reaction superiority label smoothing strategy

Variables	High superiority	Low superiority
Reaction Yield (%)	$0.05 * \frac{\text{yield} - 90}{10.0}$ (90 <= Yield <= 100)	$0.05 * \frac{\text{yield}}{50.0}$ (Yield < 50)
Reaction Time (h)	$0.05 * \frac{4 - \text{time}}{4.0}$ (time < 4)	$0.05 - 0.03 * \frac{\text{time} - 4}{8.0}$ (4 <= time < 12) $0.02 - 0.02 * \frac{\text{time} - 12}{\text{Max} - 12}$ (time >= 12)
Reaction Temperature (°C)	0.0 (15 <= Temperature <= 30)	$0.05 - 0.05 * \frac{T - 30}{\text{Max} - 30}$ (Temperature > 100) $0.05 * \frac{T - 15}{\text{Min} - 15}$ (Temperature < -10) 0.05 (-10 <= Temperature <= 100)

2.2.4 Reaction representation

Reaction representation directly affects the accuracy of the model prediction. In this work, a new condensed hypergraph reaction descriptor is proposed consisting of graph adjacency matrix and feature matrix. Graph adjacency matrix is used to describe the connection of nodes. It consists of reaction mapping graph, reaction agent graph, molecular/reaction node and reaction summary node (**Fig.1(b)**). Reaction mapping graph is constructed by the union of reactants and products graph. It considers the reaction atom transfers which provides more features for model prediction than directly splicing of molecules descriptors. Reaction agent graph uses graph data structure to represent reaction agents. In order to consider the influence between reactions and reaction agents, molecules and reaction nodes are connected to each other via bidirectional edges, enabling the message passing between reaction and agent graphs. Accompanied by bidirectional edge connections of reaction nodes and molecular nodes, the message transfer between reaction mapping graph and agent graphs are achieved. Accompanied by uni-directional edge connections of molecules and reaction nodes to reaction summary nodes, reaction features are aggregated from molecules to the whole reaction.

Node feature matrix is composed of atomic features which can be classified as indicators and change sites. Indicator sites primarily display the type of atoms, while change sites integrate the features from reactants and products to illustrate the changes in atom properties during the reactions. Edge feature matrix is composed of bond features. It is exclusively constructed by the change sites. By comparing of the bond features of the reactants and products, the changes of bond properties become clear, allowing for a clear differentiation between the directions of reversible reactions. The type of atom features and bond features are listed in **Table 1**.

Table 1. Atom features and bond features used in reaction graph descriptor

	Feature type	Feature number
Node Feature – indicator sites	Atomic type	72
Node Feature – change sites	Hybridization type	7 * 2
	Atomic charge	8 * 2
	Number of atomic connections	7 * 2
	Atomic implicit valence	7 * 2
	Total atomic valence	7 * 2
	Atomic aromaticity	1 * 2
	Atomic chirality	4 * 2
	Is the atom on the ring	6 * 2
	Number of free radicals	2 * 2
	H-atom donor/acceptor	2 * 2
	Atomic acidity/ basicity	2 * 2
Bond Feature – change sites	Bond type	4 * 2
	Is the bond on the ring	1 * 2
	Conjugate bond	1 * 2
	Chirality of bond	4 * 2

2.3 Construction of reaction superiority classification model

The reaction classification model is constructed to determine reaction superiority for reaction pathway design/selection. According to the above reaction superiority constraints, most of reaction data are unlabeled. Thus, the model trained only by labelled data may not have good generalization capability on unknown reactions. Therefore, it is necessary to utilize unsupervised methods to extract differences between reaction graph data structures for representation learning. In this work, the unlabeled data is used to construct a reaction superiority classification model through the pre-training and fine-tuning method, enhancing both prediction accuracy and generalization ability.

2.3.1 Reaction graph data augmentation algorithm

According to the model structure in **Fig.1(c)**, data augmentation plays an important role in contrastive learning which will directly affect the model training. Since most of the traditional graph data augmentation algorithms³⁴ would destroy the reaction or molecule structure and the rationality of reaction representation³⁶, a data augmentation algorithm is proposed to generate reactions with similar properties under the assumption of ignoring the carbon atom not directly connected to the reacted atoms by ignoring steric effect. The main operation of this algorithm is adding or deleting the carbon atom not directly connected to the reacted atoms. By associating this method with feature masking augmentation, the diversity of samples is increased without changing the rationality of the reaction representation. The algorithm is divided into three steps.

Step 1: Carbon addition and subtraction. Under the assumption of ignoring the influence of steric effect caused by the carbon atoms not directly connected to reacting atoms, the addition or deletion of straight chains with fewer than 3 carbon atoms to non-reactive atoms will not affect the reaction. Following the identification of manipulatable atomic nodes, carbon atoms are added to or removed from the reactant and product molecules using Rdkit⁴¹, generating novel molecular structures.

Step 2: Mapping of reaction atoms index. Since there is no mapping index number for the carbon or hydrogen atoms in the newly added straight chain, we supplement the mapping relationships of the newly added atoms in the reactions based on the neighbor information of the modified atoms, ensuring correct mapping relationship among reaction atoms.

Step 3: Molecule and atom mapping index standardization. After completing all atoms mapping index in the reaction, the molecular and atomic numbers are normalized to make the resulting reac-

tion SMARTS representations more rigorous. By reordering all the mappings index and renormalizing the molecules SMARTS, a standardized SMARTS representation of the reaction is generated to facilitate the generation of augmented reaction graph for contrastive learning.

2.3.2 Pre-training model with contrastive learning

In the pre-training process, the contrastive learning model is utilized to train the initial parameters of the backbone model using a large number of unlabeled reaction data. Negative sample-based comparison methods are often applied for molecular contrastive learning models in recent years³³⁻³⁷. Here, the SIMCLR⁴² structure contrastive learning model is used. The SIMCLR structure contains three parts, namely encoder, decoder and loss function.

The encoder part is constructed by the backbone model designed for extracting features from reaction graphs. To maximum characterization capability of GNN for graph classification, the Graph Isomorphism Network with Edge features (GINE)⁴³ constructed in DGL⁴⁴ is selected as the backbone propagation module for contrastive learning. With MLP node feature updating function, the inclusion of the AIR residual⁴⁵ and the acquisition of reaction summary node features as the readout function, the reaction summary node feature provides a unique representation of chemical reactions. The formula for GINE message passing is shown in Eq. (1).

$$\overline{h_i^{(l+1)}} = \overline{f_\theta((1 + \epsilon) h_i^{(l)} + \sum_{j \in N(i)} ReLU(h_j^{(l)} + e_{j,i}^{(l)}))} \quad (1)$$

where $h_i^{(l+1)}$ means the i 's node feature after $l + 1$ times aggregation, f_θ means the function used in updating node features, $e_{j,i}^{(l)}$ is the edge feature between node i and j after l times aggregation, ϵ is learnable parameter to control last times aggregation features influence during the message passing operation.

The decoder part utilizes the MLP for data transformation of the reaction information extracted from the backbone model. In this model framework, the data augmented from the same samples are considered as positive samples, while the different ones are considered as negative samples. To maximum the difference between positive and negative examples, and minimize the difference between positives ones, the normalized temperature-scaled cross-entropy (NT-Xent) loss⁴² is used as contrastive learning loss. The formula of NT-Xent loss is shown in Eq. (2) and (3).

$$\overline{\text{sim}(u, v)} = \overline{\frac{u^T v}{\|u\| \|v\|}} = \overline{\hat{u}^T \hat{v}} \quad (2)$$

$$\overline{l_{i,j}} = \overline{-\log \frac{\exp(\text{sim}(z_i, z_j)/\tau)}{\sum_{k=1}^{2N} \exp(\text{sim}(z_i, z_k)/\tau)}} \quad (3)$$

where $\text{sim}(u, v)$ denotes the cosine similarity between vector u and v , $l_{i,j}$ denotes the loss between i and j , and τ denotes the temperature coefficient to control the confident of SoftMax prediction.

2.3.3 Supervised learning fine-tuning model

The Reaction Superiority Classification fine-tuning model is constructed by the pre-trained backbone model and the MLP with a Sigmoid activation function is used for generating the reaction superiority probability. Since focal loss allows the model to focus more on hard negative samples, the binary focal loss⁴⁶ is selected as the loss function for fine-tuning to improve the classification accuracy of the model. The formula of binary focal loss (FL) is shown in Eq. (4).

$$\overline{\text{FL}(p_t)} = \overline{-\alpha_t (1 - p_t)^\gamma \log(p_t) - (1 - \alpha_t) p_t^\gamma \log(1 - p_t)} \quad (4)$$

where α_t is the balanced factor to solve category imbalances, γ is the focusing factor to control the model focus on hard negative samples, p_t is the positive probability predicted by the model.

After dividing the training set, validation set, and test set in accordance with 8:1:1 for model fine-tuning operations. The parameters of the backbone model and the newly constructed MLP layers are optimized using supervised learning methods. After mapping the output values to the interval from 0 to 1 using the Sigmoid activation function, the superiority probability of the reaction is generated to evaluate the reactions.

2.3.4 Details of model implementation

The pre-training model (**Fig. 1(c)**) uses the SGD⁴⁷ optimizer to optimize the parameters of backbone encoder model and projection head. The initial learning rate for backbone model pre-training process is set to 0.01 with cosine learning rate decay. It includes one warm-up epoch. The weight decay is set to 0.0005 and the momentum is set to 0.9 which can improve the prediction accuracy and learning efficiency. The total epoch number for model pre-training is 8 with a batch size 512, providing initial parameters for backbone model.

The fine-tuning model (**Fig. 1(d)**) uses the Adam⁴⁷ optimizer for gradient decent optimization. The initial learning rate for model fine-tuning is set to 0.001 with cosine learning rate decay, and the weight decay is set to 0.00001. The total number of epochs is controlled by the early stop strategy. Training is terminated when there is no improvement in accuracy in the validation set for 20 consecutive times with a batch size 256.

The backbone model is constructed with a depth of 5 GINE layers with 0.1 possibility of dropout. The hidden dimension of this backbone model is set to 300 and its readout dimension is 512. Through fully connected layers constructed in the fine-tune process with hidden dimension 256 and a dropout rate 0.5, the model could be trained to predict reaction superiority possibility easily.

3. Results and discussion

3.1 Performance evaluation

In order to show the model performance on the reaction superiority classification task, the accuracy, precision, recall, F1-score and the area under receiver operating characteristic curve (ROC-AUC) are adopted as evaluation metrics. In this work, the developed model is compared with other models by examining their performance with different message aggregation methods and investigating the utilization of the AIR residual in exploring the appropriate structure in the backbone model. The testing set evaluation results of all models are shown in **Table 4**. And the structure and training parameters of the baseline models are detailed in **Supplementary Information**.

Table 4. Reaction Superiority Classification model evaluation metrics

Model	Accuracy	Precision	Recall	F1-score	ROC-AUC
GCN-None	0.853	0.836	0.860	0.848	0.927
GAT-None	0.864	0.840	0.883	0.861	0.912
SAGE-None	0.865	0.864	0.866	0.865	0.936
GINE-None	0.884	0.852	0.921	0.885	0.940
GCN-AIR	0.876	0.853	0.905	0.878	0.920
GAT-AIR	0.871	0.844	0.905	0.873	0.942
SAGE-AIR	0.877	0.857	0.905	0.880	0.942
GINE-AIR	0.897	0.875	0.922	0.898	0.951

Model	Accuracy	Precision	Recall	F1-score	ROC-AUC
GINE-AIR with pre-training	0.903	0.898	0.908	0.903	0.965

According to the comparison of the model evaluation results presented in **Fig. 4(a)**, the backbone Model with GINE aggregation method and AIR residual shows the best performance among the several directly trained ones, where the accuracy, F1-score and ROC-AUC were 0.897, 0.898 and 0.951, respectively. It indicates that the backbone model, equipped with the GINE layers and the AIR residual, is effective in extracting more robust features for distinguishing reactions superiority. The testing set ROC curves of different models are shown in **Fig. 4(b)**, which indicate the generalization ability and prediction accuracy of the model pre-trained using contrastive learning method are significantly better than those of the direct training ones. The accuracy, F1-score and ROC-AUC of the model with contrastive learning pre-training are 0.903, 0.903 and 0.965, respectively, which shows that the pre-training via contrastive learning method can effectively improve the generalization ability of the model.

To visualize the effect of feature extraction by the pre-trained backbone model and the corresponding data space, the features extracted from the reactions are projected into 2 dimensions using Uniform Manifold Approximation and Projection (UMAP)⁴⁸ which is plotted in **Fig. 4(c)**. By analyzing the distributions of superior and inferior reaction data points, a clear distinction can be observed between the main distributions of superior and inferior reactions, indicating that the pre-trained with contrastive learning model performs better in distinguishing the reaction superiority and providing suitable advice for reaction selections.

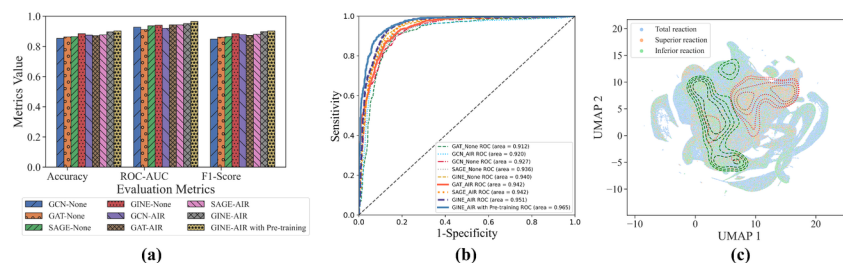


Fig. 4: Model evaluation comparison and visualization of the backbone model extraction effect

3.2 Case studies for reaction evaluation

Here, three types of reaction examples are used to illustrate the effectiveness of RSscore. (**Fig. 5**) First, the synthetic reactions of the rivaroxaban intermediate (4-phenylmorpholin-3-one) is employed as an example to evaluate the RSscore for reactions with same class. (See **Fig. 5(a)**, **Fig. 5(b)**) The substitution reactions depicted in **Fig. 5(a)** and **5(b)** allow for a straightforward analysis of reaction superiority through the leaving group effect. Except for the same leaving part, the basicity of the chloride leaving group in **Fig. 5(a)** is lower than the basicity of the ethyl ester group in **Fig. 5(b)**. It indicates that the corresponding anion of the **Fig. 5(a)** reaction leaving group is more stable, leading to milder reaction conditions in the **Fig. 5(a)** reaction. According to the experiment data from the Reaxys database, the **Fig. 5(a)** reaction demonstrates the same reaction temperature, a higher reaction yield and a shorter reaction time compared to the **Fig. 5(b)** reaction. It validates the leaving group effect and indicates that the **Fig. 5(a)** reaction exhibits higher superiority. In accordance of the evaluation metric proposed in this paper, the RSscore achieved 0.7939 in **Fig. 5(a)** and 0.7651 in **Fig. 5(b)**. It indicates that the **Fig. 5(a)** reaction exhibits a higher reaction superiority, aligning with the results obtained from the experimental and mechanistic

analyses. This demonstrates that the RSscore can detect the impact of electronic effects, and effectively distinguishes the superiority differences among reactions within the same class.

Synthetic reactions of Pomalidomide intermediate (4-nitrothalidomide) using different reaction agents are conducted to determine whether the RSscore can detect the impact of the reaction agent. The experimental data shows that the reaction using **Fig. 5(c)** agents exhibit lower reaction time, higher reaction yield and milder reaction temperature condition compared to the reaction using **Fig. 5(d)** agents. After completing the reaction atom mapping, the RSscore for reactions using **Fig. 5(c)** and **Fig. 5(d)** agents are calculated as 0.7518 and 0.4812, respectively. This demonstrates that the RSscore are consistent with experimental data and provide a better reflection of the reaction agents influence on chemical reactions.

Finally, as an exploration of the assessment effect of the RSscore in different reactions, the synthesis reactions Olaparib intermediate (4-(4-fluoro-3-(piperazine-1-carbonyl)benzyl)phthalazin-1(2H)-one) are used as an example for comparison. Although the final product and the reacted sites for the reactions in **Fig. 5(e)** and **Fig. 5(f)** are the same, the reaction type are completely different, with **Fig. 5(e)** being a hydrolysis reaction and **Fig. 5(f)** being a condensation reaction. Based on the comparison of the experimental data between the reactions in **Fig. 5(e)** and **Fig. 5(f)**, the reaction in **Fig. 5(e)** is superior in terms of reaction time, yield, and temperature condition. The calculated RSscore for **Fig. 5(e)** is 0.7836 and for **Fig. 5(f)** is 0.6399. The magnitude relationship of the RSscore supports the superiority of the reaction in **Fig. 5(e)**, which aligns with the experimental data.

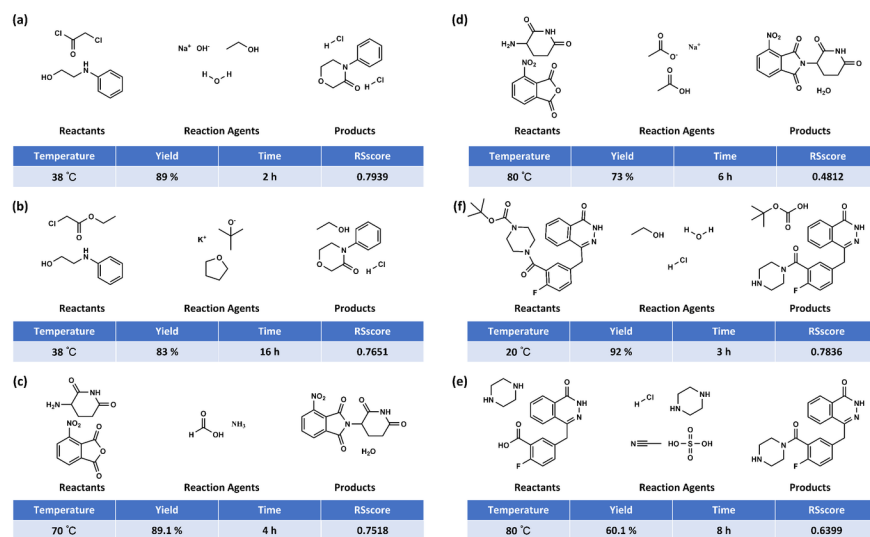


Fig. 5 The effectiveness test of the RSscore on reaction evaluation

Each indicator is evaluated separately in the external test set to demonstrate the generalizability and superiority. According to the evaluation indicators results in **Table 5**, the RSscore exhibits the highest accuracy (accuracy = 0.717) and ROC-AUC value (ROC-AUC = 0.714) among these indicators. The generalizability and superiority of RSscore are proved in discriminating the superior situations of reactions. Furthermore, when considering reactions carried out with different reaction agents, only RSscore can distinguish those reactions. This demonstrates the broader capability of RSscore to judge reaction superiority and provides a good evaluation indicator for CASP.

Table 5. Reaction evaluation indicators on external test set

Evaluation indicators	Accuracy	Precision	Recall	F1-Score	ROC-AUC	Reaction Agent Recognition
SAscore	0.473	0.478	0.594	0.530	0.473	N

Evaluation indicators	Accuracy	Precision	Recall	F1-Score	ROC-AUC	Reaction Agent Recognition
SCscore	0.465	0.476	0.703	0.568	0.465	N
RAscore	0.486	0.484	0.437	0.459	0.486	N
GASA	0.481	0.467	0.277	0.348	0.481	N
SYBA	0.496	0.490	0.200	0.284	0.496	N
RSscore	0.717	0.699	0.761	0.729	0.714	Y

Here, to further illustrate the advantage of RSscore over other evaluation indicators based on molecular accessibility and complexity, we take the reaction in **Fig. 5(a)** as an example and obtained the evaluation results in **Table 6** ., the RSscore has consistent result with SAScore, SCscore, SYBA, RAscore, at the same time, it is able to consider the effect of reaction agents, enabling the identification of the current reaction as a relatively dominant one. This demonstrates the broader capability of RSscore to judge reaction superiority and provides a good evaluation indicator for CASP.

Table 6. Reaction evaluation indicators on reaction

Evaluation indicators	Reactant Score	Product Score	Reaction Score	Reaction Agent Recognition	Reaction Type
SAscore	1.4682	1.8126	-	N	Superior
SCscore	1.6092	2.2959	-	N	Superior
RAscore	0.9956	0.9785	-	N	Superior
GASA	0.8810	0.9391	-	N	Inferior
SYBA	41.0929	20.7120	-	N	Superior
RSscore	-	-	0.7939	Y	Superior

3.3 Application in synthetic routes analysis

To study the effectiveness of RSscore in synthetic routes analysis, we utilized three synthetic routes of paracetamol for validation. As all three synthetic routes utilize the reaction of p-aminophenol with acetic acid at the end of paracetamol synthesis routes, its overall impact on synthetic route is negligible. After obtaining the reaction condense hypergraph descriptors and calculating the RSscore of each reaction of the synthetic routes in **Fig. 6** , the RSscore for reactions in route (a) are 0.7430 and 0.5587; the RSscore for reactions in route (b) are 0.6535 and 0.4492, and the RSscore for reactions in route (c) are 0.7569 and 0.5867, respectively. By comparing the RSscore values of the reaction in the synthetic routes, the reactions in route (a) and (c) exhibit better overall performance compared to the route (b). This demonstrates that synthetic route (a) and (c) are more favorable than route (b) in terms of the combination of reaction time, yield and temperature condition.

In practical studies of these synthetic pathways, Route (a) has the advantages of short reaction time and high yield.⁴⁹Route (b) requires fewer steps, but the yield for the p-aminophenol generation is low, while the handling of the waste residue generated is difficult. Therefore, this synthesis method has been abandoned by many countries.⁵⁰ Route (c) could generate a high-quality of p-aminophenol, and its yield can reach 72%.⁵⁰Through a comparison of synthetic routes, Routes (a) and Routes (c) are relatively better and perform little difference on reaction yield, time and temperature conditions. Although the cost for Route (c) is cheaper than Route (a), the price factor is not involved in the proposed indicator, therefore the RSscore is not able to distinguish the difference between the two routes.

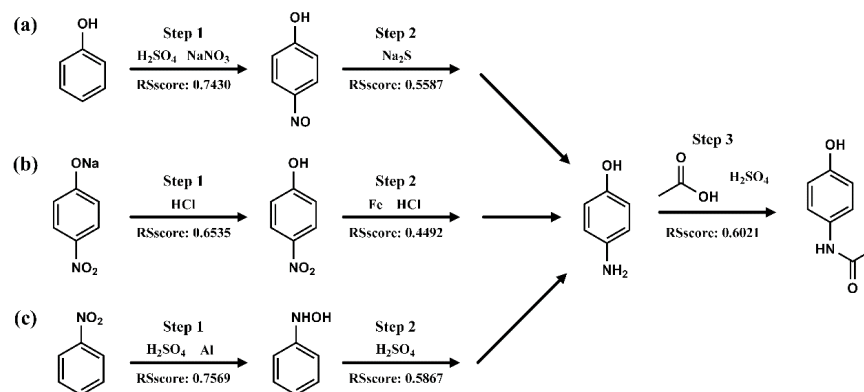


Fig. 6. The effectiveness test of the RScore on Paracetamol synthetic routes analysis

Another validation example is also given here for Clobazam synthesis routes. After obtaining the reaction condense hypergraph descriptors and calculating the average RScore of each reaction synthetic routes in **Fig. 7**, the average RScore for route (a), (b) and (c) are 0.5915, 0.7493 and 0.7721, respectively. By comparing the average RScore values of the synthetic routes, the reactions in route (b) and (c) exhibit better overall performance compared to the route (a). This demonstrates that synthetic route (b) and (c) are more favorable than route (a) in terms of the combination of reaction time, yield and temperature condition.

In practical studies of these synthetic pathways, Route (a) has longer reaction steps and low yield (total yield can reach approximate 11%).⁵¹ Route (b) and Route (c) require fewer steps and the yield for each step in Clobazam generation are high (total yield can reach approximate 50%) which provides a methodology for the industrial production of clobazam.^{52,53} Through a comparison of the synthetic routes from literature results, Route (b) and Route (c) are relatively better. However, Route (b) requires hydrogenation reaction equipment, which results in higher production cost than Routes (c). According to the development of RScore, the production cost is not considered. Therefore, the RScore is not able to distinguish the difference between the Route (b) and Route (c). The comparison result of the synthetic routes is consistent with the conclusions obtained by RScore, which shows that RScore can be a better aid to the analysis of the synthetic routes.

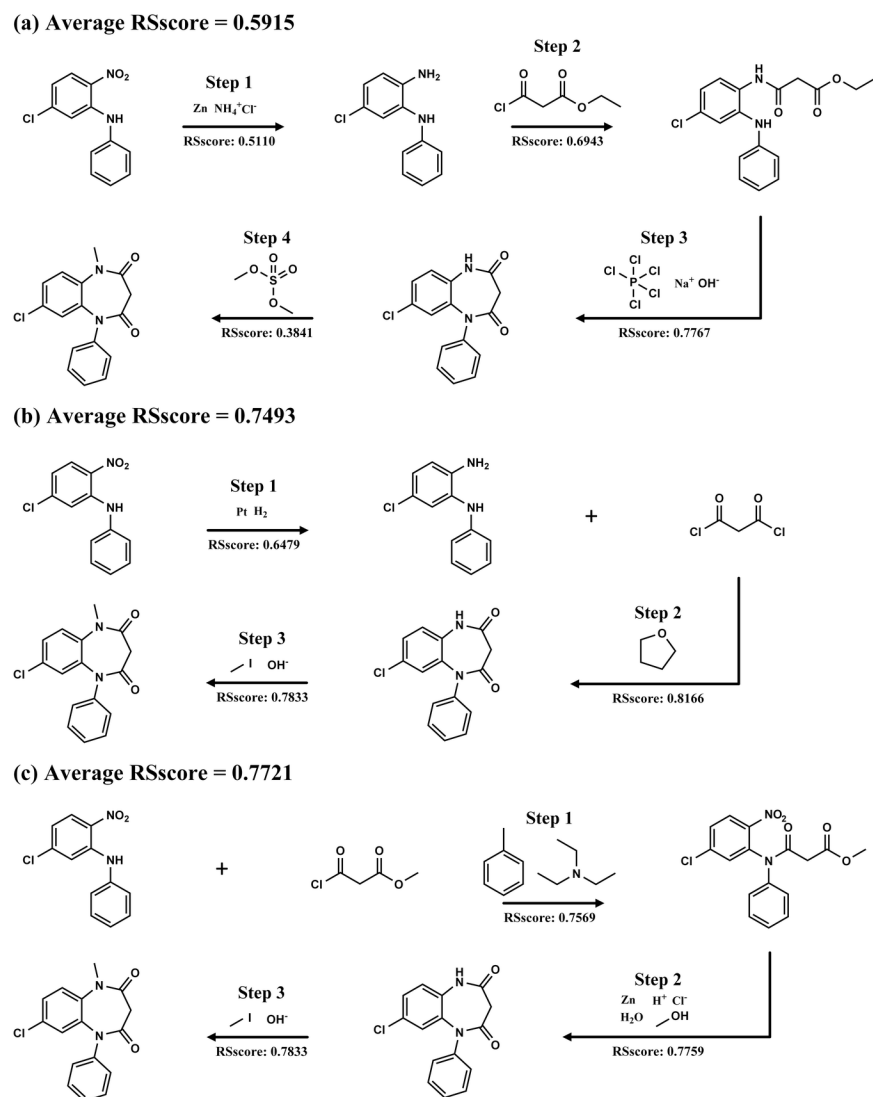


Fig. 7. The effectiveness test of the RSscore on Clobazam synthetic routes analysis

4. Data Availability and Reproducibility Statement

Firstly, all codes needed to get RSscore are available at <https://gitee.com/xu-chenyang/rsscore>. The results of the RTAAM in **Fig. 2** can be obtained by the programme in the /Data_Prepare&Augmentation/RTAAM directory of RSscore code and the details of RTAAM algorithm are shown in section S1 of the Supplementary Material. For the reaction representation features in Table 1, more details on reaction representation features are shown in section S2 of the Supplementary Material. The distribution of the reaction yield in **Fig. 3** is obtained by the USPTO data in the ORD³⁹ database with complete yield, temperature and time information. In **Fig. 4(a)** and **4(b)**, the bar plot and ROC curve are drawn based on the results of the model evaluation in **Table 4** used to indicate the advantages difference between different models, the specific construction method and model performance are shown in section S3 of the Supplementary Material. In **Fig. 4(c)**, the result of the superior and inferior reaction data distribution is drawn by the trained UMAP model. The

reaction feature arrays are clustered by UMAP are shown under the /UMAP directory.

The evaluated reactions in **Fig. 5** were achieved from Reaxys²², and the RSScore calculation can be obtained in /reaction_evaluation directory of RSScore code. The synthetic routes analysis in **Fig. 6** and **Fig. 7** can be obtained from patents⁵¹⁻⁵³ and articles^{49,50}. The RSScore calculation can be obtained in /synthetic_route_analysis directory of RSScore code.

5. Conclusions

In this paper, we developed a novel chemical reaction superiority evaluation index based on the information from the reaction database using deep learning (DL) methods. For the modeling of RSScore, a new type of chemical reaction graph descriptor with atom mapping relationship was constructed, which provides sufficient chemical reaction information and significantly improved the model classification ability. Label smoothing was also employed to reduce the overfitting of the model and enable differentiation of reaction superiority within the same categories. Contrastive learning pre-training and supervised learning fine-tuning method were used to improve the generality of the model and the accuracy of classification.

The effect of different message passing methods was investigated and the AIR residual on the GNN model is used to generate the RSScore. It proves that the GINE message passing methods combined with AIR residual demonstrate the best outcomes on classification. Additionally, the data distribution of the entire dataset is analyzed and visualized using UMAP dimensionality reduction, which showed that the developed model effectively distinguishes reaction superiority and generates a robust evaluation metric. The effectiveness of this RSScore provides a crucial evaluation index for the computer-aided synthesis planning.

ASSOCIATED CONTENT

Supplementary Material .

The **Supplementary Material** is available free of charge.

AUTHOR INFORMATION

Corresponding Author

*Lei Zhang: E-mail addresses: keleiz@dlut.edu.cn

Author Contributions

Chenyang Xu : conceptualization; data curation; investigation; methodology; validation; visualization; writing-original draft; writing-review and editing. **Lijuan Guo** : writing-review and editing. **Lei Zhang**: conceptualization; funding acquisition; resources; supervision; writing-review and editing.

Code availability

All codes needed to get RSScore are available at <https://gitee.com/xu-chenyang/rsscore>

ACKNOWLEDGMENT

The authors are grateful for the financial support of NSFC (22078041, 22278053), Dalian High-level Talents Innovation Support Program (2021RQ105) and the fundamental Research Funds for China Central Universities (DUT22QN209, DUT22LAB608).

REFERENCES

1. Tan D, Friščić T. Mechanochemistry for Organic Chemists: An Update. *European Journal of Organic Chemistry* . 2018;2018(1):18-33.
2. Ihlenfeldt W-D, Gasteiger J. Computer-Assisted Planning of Organic Syntheses: The Second Generation of Programs. *Angewandte Chemie International Edition in English* . 1996;34(2324):2613-2633.
3. Engkvist O, Norrby P-O, Selmi N, et al. Computational prediction of chemical reactions: current status and outlook. *Drug Discovery Today* . 2018;23(6):1203-1218.
4. Coley CW, Green WH, Jensen KF. Machine Learning in Computer-Aided Synthesis Planning. *Accounts of Chemical Research* . 2018;51(5):1281-1289.
5. Baskin II, Madzhidov TI, Antipin IS, Varnek AA. Artificial intelligence in synthetic chemistry: achievements and prospects. *Russian Chemical Reviews* . 2017;86(11):1127-1156.
6. Szymkuć S, Gajewska EP, Klucznik T, et al. Computer-Assisted Synthetic Planning: The End of the Beginning. *Angewandte Chemie International Edition* . 2016;55(20):5904-5937.
7. Skoraczyński G, Kitlas M, Miasojedow B, Gambin A. Critical assessment of synthetic accessibility scores in computer-assisted synthesis planning. *Journal of Cheminformatics* . 2023;15(1).
8. Qiu F. Strategic efficiency — The new thrust for synthetic organic chemists. *Canadian Journal of Chemistry* . 2008;86(9):903-906.
9. Ito S, Baba Y, Isomura T, Kashima H. Synthetic accessibility assessment using auxiliary responses. *Expert Systems with Applications* . 2020;145.
10. Podolyan Y, Walters MA, Karypis G. Assessing Synthetic Accessibility of Chemical Compounds Using Machine Learning Methods. *Journal of Chemical Information and Modeling* . 2010/06/28 2010;50(6):979-991.
11. Fukunishi Y, Kurosawa T, Mikami Y, Nakamura H. Prediction of Synthetic Accessibility Based on Commercially Available Compound Databases. *Journal of Chemical Information and Modeling* . 2014;54(12):3259-3267.
12. Li B, Chen H. Prediction of Compound Synthesis Accessibility Based on Reaction Knowledge Graph. *Molecules* . 2022;27(3).
13. Ertl P, Schuffenhauer A. Estimation of synthetic accessibility score of drug-like molecules based on molecular complexity and fragment contributions. *Journal of Cheminformatics* . 2009;1(1).
14. Coley CW, Rogers L, Green WH, Jensen KF. SCScore: Synthetic Complexity Learned from a Reaction Corpus. *Journal of Chemical Information and Modeling* . 2018;58(2):252-261.
15. Voršilák M, Kolář M, Čmelo I, Svozil D. SYBA: Bayesian estimation of synthetic accessibility of organic compounds. *Journal of Cheminformatics* . 2020;12(1).
16. Thakkar A, Chadimová V, Bjerrum EJ, Engkvist O, Reymond J-L. Retrosynthetic accessibility score (RAscore) – rapid machine learned synthesizability classification from AI driven retrosynthetic planning. *Chemical Science* . 2021;12(9):3339-3349.

17. Yu J, Wang J, Zhao H, et al. Organic Compound Synthetic Accessibility Prediction Based on the Graph Attention Mechanism. *Journal of Chemical Information and Modeling* . 2022;62(12):2973-2986.
18. Rogers D, Hahn M. Extended-Connectivity Fingerprints. *Journal of Chemical Information and Modeling* . 2010/05/24 2010;50(5):742-754.
19. Kim S, Chen J, Cheng T, et al. PubChem 2019 update: improved access to chemical data. *Nucleic Acids Research* . 2019;47(D1):D1102-D1109.
20. Wang W, Liu Q, Zhang L, Dong Y, Du J. RetroSynX: A retrosynthetic analysis framework using hybrid reaction templates and group contribution-based thermodynamic models. *Chemical Engineering Science* . 2022;248.
21. Gao W, Coley CW. The Synthesizability of Molecules Proposed by Generative Models. *Journal of Chemical Information and Modeling* . 2020;60(12):5714-5723.
22. Reaxys. <https://www.reaxys.com>. Accessed August 19, 2023. <https://www.reaxys.com>
23. Andraos J. Aiming for a standardized protocol for preparing a process green synthesis report and for ranking multiple synthesis plans to a common target product. *Green Processing and Synthesis* . 2019;8(1):787-801.
24. Chen B, Li C, Dai H, Song L. Retro*: Learning Retrosynthetic Planning with Neural Guided A* Search. 2020:arXiv:2006.15820.
25. Genheden S, Thakkar A, Chadimová V, Reymond J-L, Engkvist O, Bjerrum E. AiZynthFinder: a fast, robust and flexible open-source software for retrosynthetic planning. *Journal of Cheminformatics* . 2020;12(1).
26. Gilmer J, Schoenholz SS, Riley PF, Vinyals O, Dahl GE. Neural Message Passing for Quantum Chemistry. 2017:arXiv:1704.01212.
27. Schütt KT, Sauceda HE, Kindermans PJ, Tkatchenko A, Müller KR. SchNet - A deep learning architecture for molecules and materials. *The Journal of chemical physics* . Jun 28 2018;148(24):241722.
28. Yang J, Liu Z, Xiao S, et al. GraphFormers: GNN-nested Transformers for Representation Learning on Textual Graph. 2021:arXiv:2105.02605.
29. Shui Z, Karypis G. Heterogeneous Molecular Graph Neural Networks for Predicting Molecule Properties. presented at: 2020 IEEE International Conference on Data Mining (ICDM); 2020;
30. Li Y, Zhang L, Liu Z. Multi-Objective De Novo Drug Design with Conditional Graph Generative Model. 2018:arXiv:1801.07299.
31. Li Y, Vinyals O, Dyer C, Pascanu R, Battaglia P. Learning Deep Generative Models of Graphs. 2018:arXiv:1803.03324.
32. You J, Liu B, Ying R, Pande V, Leskovec J. Graph Convolutional Policy Network for Goal-Directed Molecular Graph Generation. 2018:arXiv:1806.02473.
33. Pinheiro GA, Da Silva JLF, Quiles MG. SMICLR: Contrastive Learning on Multiple Molecular Representations for Semisupervised and Unsupervised Representation Learning. *Journal of Chemical Information and Modeling* . 2022;62(17):3948-3960.
34. Wang Y, Wang J, Cao Z, Barati Farimani A. Molecular contrastive learning of representations via graph neural networks. *Nature Machine Intelligence* . 2022/03/01 2022;4(3):279-287.
35. Li S, Zhou J, Xu T, Dou D, Xiong H. GeomGCL: Geometric Graph Contrastive Learning for Molecular Property Prediction. 2021:arXiv:2109.11730.

36. Sun M, Xing J, Wang H, Chen B, Zhou J. MoCL: Data-driven Molecular Fingerprint via Knowledge-aware Contrastive Learning from Molecular Graph. presented at: Proceedings of the 27th ACM SIGKDD Conference on Knowledge Discovery & Data Mining; 2021;
37. Fang Y, Zhang Q, Yang H, et al. Molecular Contrastive Learning with Chemical Element Knowledge Graph. 2021:arXiv:2112.00544.
38. Kwon Y, Lee D, Choi Y-S, Kang S. Uncertainty-aware prediction of chemical reaction yields with graph neural networks. *Journal of Cheminformatics* . 2022;14(1).
39. Kearnes SM, Maser MR, Wlekliniski M, et al. The Open Reaction Database. *Journal of the American Chemical Society* . 2021;143(45):18820-18826.
40. Vaucher AC, Zipoli F, Geluykens J, Nair VH, Schwaller P, Laino T. Automated extraction of chemical synthesis actions from experimental procedures. *Nature Communications* . 2020;11(1).
41. Landrum G. Rdkit: Open-source chemoinformatics and machine learning. . Accessed August 19, 2023.<http://rdkit.org>
42. Chen T, Kornblith S, Norouzi M, Hinton G. A Simple Framework for Contrastive Learning of Visual Representations. 2020:arXiv:2002.05709.
43. Hu W, Liu B, Gomes J, et al. Strategies for Pre-training Graph Neural Networks. 2019:arXiv:1905.12265.
44. Deep graph library.<https://www.dgl.ai>. Accessed August 19, 2023.
45. Zhang W, Sheng Z, Yin Z, et al. Model Degradation Hinders Deep Graph Neural Networks. presented at: Proceedings of the 28th ACM SIGKDD Conference on Knowledge Discovery and Data Mining; 2022;
46. Lin T-Y, Goyal P, Girshick R, He K, Dollár P. Focal Loss for Dense Object Detection. 2017:arXiv:1708.02002.
47. Ruder S. An overview of gradient descent optimization algorithms. 2016:arXiv:1609.04747.
48. McInnes L, Healy J, Melville J. UMAP: Uniform Manifold Approximation and Projection for Dimension Reduction. 2018:arXiv:1802.03426.
49. Yanqiong G. Study on Synthesis of Paracetamol. *JOURNAL OF GUANGDONG UNIVERSITY OF TECHNOLOGY* . 1997;
50. Si-Yi LI, You-Zhi L, Qiao-Ling Z, Mei B. Review on preparation methods of p-aminophenol. *Fine and Specialty Chemicals* . 2011;
51. Kumar AV, Kiritkumar SD, Kantibhai PR, Rajendrakumar PB, Mansukhlal TN, Rameshchandra UA. PROCESS FOR PREPARING CLOBAZAM USING NOVEL INTERMEDIATES. 2016.
52. Fang Y, Du Y. A method for the preparation of clobazam. 2017.
53. Zhou H, Peng C, Liu Q, Zhang Z, Liao Z. A method for the industrial production of clobazam. 2021.